Pharm Res
https://doi.org/10.1007/s11095-021-03078-w

RESEARCH PAPER

Revising Pharmacokinetics of Oral Drug Absorption: II Bioavailability-Bioequivalence Considerations

Pavlos Chryssafidis [1,2] • Athanasios A. Tsekouras [3,1] • Panos Macheras [1,2]

Received: 9 May 2021 / Accepted: 28 June 2021

ABSTRACT

Purpose To explore the application of the parameters of the physiologically based finite time pharmacokinetic (PBFTPK) models subdivided in first-order $(PBFTPK)_1$ and zero-order $(PBFTPK)_0$ models to bioavailability and bioequivalence. To develop a methodology for the estimation of absolute bioavailability, *F*, from oral data exclusively.

Methods Simulated concentration time data were generated from the Bateman equation and compared with data generated from the $(PBFTPK)_1$ and $(PBFTPK)_0$ models. The blood concentration $C_b(\tau)$ at the end of the absorption process τ, was compared to C_{max}; the utility of $(AUC)_0^{\tau}$ and $(AUC)_t^{\infty}$ in bioequivalence assessment was also explored. Equations for the calculation of *F* from oral data were derived for the $(PBFTPK)_1$ and $(PBFTPK)_0$ models. An estimate for *F* was also derived from an areas proportionality using oral data exclusively.

Results The simulated data of the $(PBFTPK)_0$ models exhibit rich dynamics encountered in complex drug absorption phenomena. Both $(PBFTPK)_1$ and $(PBFTPK)_0$ models result either in $C_{max} = C_b(\tau)$ or $C_{max} > C_b(\tau)$ for rapidly- and not rapidly-absorbed drugs, respectively; in the latter case, $C_b(\tau)$ and τ are meaningful parameters for drug's rate of exposure. For both $(PBFTPK)_1$ and $(PBFTPK)_0$ models, $(AUC)_0^{\tau}$ or portions of it cannot be used as early exposure rate indicators. $(AUC)_{\tau}^{\infty}$ is a useful parameter for the assessment of extent of absorption for very rapidly absorbed drugs. An estimate for *F* for theophylline formulations was found close to unity.

Conclusion The $(PBFTPK)_1$ and $(PBFTPK)_0$ models are more akin to *in vivo* conditions. Estimates for *F* can be derived from oral data exclusively.

KEY WORDS Bioavailability · bioequivalence · finite time of absorption · physiologically based finite time pharmacokinetic models · physiologically based pharmacokinetic models

ABBREVIATIONS

BCS	Biopharmaceutic classification system
PBPK	Physiologically based pharmacokinetics
PBFTPK	Physiologically based finite time pharmacokinetics
RMZ	Remimazolam

INTRODUCTION

Since the early days of pharmacokinetics when Dost (1) introduced this term, first-order absorption became a dogma for all routes of drug administration, e.g., oral, nasal, muscular, pulmonary. The concept of first-order absorption and the implied infinite time for the completion of absorption process are widely applied in the contemporary pharmacokinetics, pharmacokinetics-pharmacodynamics, pharmacometric studies and relevant software packages (2, 3).

Based on common wisdom and scientific belief that "*drugs are mostly absorbed in the small intestine in finite time*", the theoretical termination of oral drug absorption at infinite time was questioned (4). The following equations based on the one compartment model were used in the simulations (4) to describe the concentration time profile until and beyond the finite time, τ corresponding to the termination of drug absorption (5, 6).

✉ Panos Macheras
macheras@pharm.uoa.gr

[1] PharmaInformatics Unit, Research Center ATHENA, Athens, Greece

[2] Faculty of Pharmacy, Laboratory of Biopharmaceutics Pharmacokinetics, National and Kapodistrian University of Athens, Athens, Greece

[3] Department of Chemistry, Laboratory of Physical Chemistry, National and Kapodistrian University of Athens, Athens, Greece

Published online: 02 August 2021

$$C_b(t) = \frac{FDk_a}{V_d(k_a - k_{el})}\left(e^{-k_{el}t} - e^{-k_a t}\right) \quad t \le \tau \tag{1}$$

$$C_b(t) = C_b(\tau)e^{-k_{el}(t-\tau)} \quad t > \tau \tag{2}$$

where $C_b(t)$ is the drug concentration in the body (compartment) at time t, F is the bioavailable fraction of dose D, V_d is the volume of distribution and k_a, k_{el} are the absorption and elimination rate constants, respectively. Time τ denotes either the passage of drug beyond the absorptive sites or the completion of the absorption process since no more dissolved drug is available for absorption (4). The model based on Eqs. 1 and 2 will be called $(PBFTPK)_1$, i.e., Physiologically Based Finite Time Pharmacokinetic model while the subscript 1 denotes that the model maintains the first order character of drug's absorption rate.

Recently, models based on biopharmaceutical/physiological and finite absorption time concepts were developed (7). For these models the term $(PBFTPK)_0$ (Physiologically Based Finite Time Pharmacokinetic) models is used herein, where the subscript 0 denotes the zero order character of drug's absorption. They were build on two principles (7) associated with the biopharmaceutic classification system (BCS) (8–10) i) drugs are absorbed passively under sink conditions for a finite period of time, τ and ii) one of the drug's properties either solubility or permeability plays the rate limiting role in drug absorption. Besides, relevant time absorption constrains linked with the gastrointestinal transit times of drug in the stomach, the small intestines and the colon were applied (7).

In this work, we present the first major application of finite time absorption concept associated with the development of $(PBFTPK)_0$ and $(PBFTPK)_1$ models. We explore the drug blood concentration at time τ, $C_b(\tau)$, as well as the partial areas under the curve, $[AUC]_0^\tau$ and $[AUC]_\tau^\infty$ prior to and beyond the termination of drug's absorption at time τ, respectively, as metrics for the assessment of drug's rate or extent of absorption. In addition, we apply the $(PBFTPK)_0$ and $(PBFTPK)_1$ models for the analysis of concentration-time data to get an estimate for the absolute bioavailablity from oral data exclusively.

THEORY

Since the first compartmental models were used in Physics for the description of radioactive decay, Dost adopted Eq.1 without any time restriction, the physicist Harry Bateman's equation (11) to describe the oral absorption of drugs, assuming a one compartment model disposition with first-order absorption and elimination rate. According to Eq.1, both absorption and elimination processes run concurrently from zero to infinity (4, 7, 11).

The development of bioavailability concepts and metrics both for the extent and rate of absorption was based on the parameters $[AUC]_0^\infty$, $C_{\max}$ and $t_{\max}$,which are derived from Eq.1 (12):

$$[AUC]_0^\infty = \frac{FD}{V_d k_{el}} = \frac{FD}{CL} \tag{3}$$

$$t_{max} = \frac{1}{k_a - k_{el}}\ln\left(\frac{k_a}{k_{el}}\right) \tag{4}$$

$$C_{max} = \frac{FD}{V_d}\left(\frac{k_a}{k_{el}}\right)^{-\left(\frac{k_{el}}{k_a - k_{el}}\right)} \tag{5}$$

where CL is the drug clearance. $[AUC]_0^\infty$ is the infinite integral of Eq.1, $C_{\max}$ and $t_{\max}$ are calculated by equating the first derivative of Eq.1 with zero.

$(PBFTPK)_0$ models

For the one-compartment model the following equation was used to describe the drug blood concentration for $t \le \tau$ assuming termination of absorption at time τ (7):

$$C_b(t) = \frac{FD}{\tau}\frac{1}{V_d k_{el}}\left(1 - e^{-k_{el}t}\right) \quad t \le \tau \tag{6}$$

while for $t > \tau$, Eq.2 applies. The drug blood concentration $C_b(\tau)$ corresponding to time τ, for the one compartment $(PBFTPK)_0$ model is derived from Eq.6 using $t = \tau$:

$$C_b(\tau) = \frac{FD}{\tau}\frac{1}{V_d k_{el}}\left(1 - e^{-k_{el}\tau}\right) = \frac{FD}{\tau}\frac{1}{CL}\left(1 - e^{-k_{el}\tau}\right) \tag{7}$$

while the areas $[AUC]_0^\tau$ and $[AUC]_\tau^\infty$ are derived by integrating Eqs. 6 and 2, respectively:

$$[AUC]_0^\tau = \frac{FD}{\tau}\frac{1}{V_d k_{el}}\left(\tau - \frac{1 - e^{-k_{el}\tau}}{k_{el}}\right) = \frac{FD}{V_d k_{el}}\left(1 - \frac{1 - e^{-mln2}}{mln2}\right) = \\ = [AUC]_0^\infty\left(1 - \frac{1 - e^{-mln2}}{mln2}\right) \tag{8}$$

where m is the ratio $(m = \tau/t_{1/2})$ of τ over the half-life $t_{1/2}$ while $k_{el} = (\ln 2)/t_{1/2}$.

$$[AUC]_\tau^\infty = \frac{C_b(\tau)}{k_{el}} = \frac{FD}{V_d k_{el}}\frac{1}{k_{el}\tau}\left(1 - e^{-k_{el}\tau}\right) \\ = [AUC]_0^\infty\frac{1}{mln2}\left(1 - e^{-mln2}\right) \tag{9}$$

The sum of the two last integrals, Eqs. 8 and 9, gives $[AUC]_0^\infty$, Eq.3.

A hypothetical curve corresponding to the same dose given as an intravenous bolus dose would follow the same track for $t \geq \tau$. Having the general form of

$$C_{biv}(t) = Ge^{-k_{el}t} \tag{10}$$

Requiring.

$$C_{biv}(t) = C_b(t) \text{ for } t \geq \tau, \tag{11}$$

we get:

$$Ge^{-k_{el}t} = C_b(\tau)e^{-k_{el}(t-\tau)} = \frac{FD}{\tau}\frac{1}{V_d k_{el}}\left(1-e^{-k_{el}\tau}\right)e^{-k_{el}(t-\tau)} \tag{12}$$

giving

$$G = \frac{FD}{\tau}\frac{1}{V_d k_{el}}\left(1-e^{-k_{el}\tau}\right)e^{k_{el}\tau} = \frac{FD}{\tau}\frac{1}{V_d k_{el}}\left(e^{k_{el}\tau}-1\right) \tag{13}$$

Then, the hypothetical curve would give:

$$[AUC_{iv}]_0^\infty = \frac{G}{k_{el}} = \frac{FD}{V_d k_{el}}\frac{1}{k_{el}\tau}\left(e^{k_{el}\tau}-1\right) = [AUC]_0^\infty \frac{1}{k_{el}\tau}\left(e^{k_{el}\tau}-1\right) \tag{14}$$

Re-arranging the last equation, we get

$$F = \frac{[AUC]_0^\infty}{[AUC_{iv}]_0^\infty} = \frac{k_{el}\tau}{e^{k_{el}\tau}-1} \tag{15}$$

Where F is the fraction of dose absorbed since both oral and intravenous data rely on a single oral administration of dose to an individual. However, if first-pass effect is not encountered, then F in Eq.9 denotes the bioavailable fraction.

Although more than one constant input rate may operate successively under *in vivo* conditions (7), this section focuses on the simplest case, i.e., the one-compartment model with constant input rate and first-order elimination. However, the concepts developed herein can be adapted to models with more than one input rate.

If two constant input rates operate successively under *in vivo* conditions, Eqs. 6 and 2 are replaced by:

$$C_b(t) = \frac{F_1 D}{\tau_1}\frac{1}{V_d k_{el}}\left(1-e^{-k_{el}t}\right) \quad 0 < t \leq \tau_1 \tag{16}$$

$$C_b(t) = C_b(\tau_1)e^{-k_{el}(t-\tau_1)} + \frac{F_2 D}{\tau_2}\frac{1}{V_d k_{el}}\left(1-e^{-k_{el}(t-\tau_1)}\right) \quad \tau_1 \leq t \leq \tau_1+\tau_2 \tag{17}$$

$$C_b(t) = C_b(\tau_1+\tau_2)e^{-k_{el}(t-\tau_1-\tau_2)} \quad \tau_1+\tau_2 < t \tag{18}$$

If three constant input rates operate successively under *in vivo* conditions, Eqs. 6 and 2 are replaced by:

$$C_b(t) = \frac{F_1 D}{\tau_1}\frac{1}{V_d k_{el}}\left(1-e^{-k_{el}t}\right) \quad 0 < t \leq \tau_1 \tag{19}$$

$$C_b(t) = C_b(\tau_1)e^{-k_{el}(t-\tau_1)} + \frac{F_2 D}{\tau_2}\frac{1}{V_d k_{el}}\left(1-e^{-k_{el}(t-\tau_1)}\right) \quad \tau_1 < t \leq \tau_1+\tau_2 \tag{20}$$

$$C_b(t) = C_b(\tau_1+\tau_2)e^{-k_{el}(t-\tau_1-\tau_2)} + \frac{F_3 D}{\tau_3}\frac{1}{V_d k_{el}}\left(1-e^{-k_{el}(t-\tau_1-\tau_2)}\right) \quad \tau_1+\tau_2 < t \leq \tau_1+\tau_2+\tau_3 \tag{21}$$

$$C_b(t) = C_b(\tau_1+\tau_2+\tau_3)e^{-k_{el}(t-\tau_1-\tau_2-\tau_3)} \quad \tau_1+\tau_2+\tau_3 < t \tag{22}$$

$(PBFTPK)_1$ models

These models rely on Eqs. 1 and 2 (4–6). Using

$$C_b(\tau) = \frac{FDk_a}{V_d(k_a-k_{el})}\left(e^{-k_{el}\tau}-e^{-k_a\tau}\right) \tag{23}$$

the areas $[AUC]_0^\tau$ and $[AUC]_\tau^\infty$ are derived by integrating Eqs. 1 and 2, respectively:

$$[AUC]_0^\tau = \frac{FD}{V_d k_{el}} - \frac{FDk_a}{V_d(k_a-k_{el})}\left(\frac{e^{-k_{el}\tau}}{k_{el}} - \frac{e^{-k_a\tau}}{k_a}\right) \tag{24}$$

$$[AUC]_\tau^\infty = \frac{C_b(\tau)}{k_{el}} = \frac{FDk_a}{V_d k_{el}(k_a-k_{el})}\left(e^{-k_{el}\tau}-e^{-k_a\tau}\right) \tag{25}$$

The sum of Eqs.24 and 25 gives

$$[AUC]_0^\infty = \frac{FD}{V_d k_{el}}\left(1-e^{-k_a\tau}\right) \tag{26}$$

The deviation of the latter quantity from the required value of $\frac{FD}{V_d k_{el}}$ is associated with the discrepancy between the physical assumption that the drug is not absorbed any more beyond time τ, and the mathematics of first-order absorption process, which lasts until infinity. In fact, the term in parentheses of Eq. 26 is linked with the absorption characteristics, i.e., the absorption rate constant k_a and the duration of absorption τ. The impact of this term becomes smaller for high values of k_a and τ, Fig. 1; the term used in the ordinate of Fig. 1 allows a dimensionless plot.

A hypothetical curve corresponding to the same dose given as an intravenous bolus dose would follow the same track for $t \geq \tau$. Having the general form of

$$C_{biv}(t) = Ge^{-k_{el}t} \tag{27}$$

Requiring.

$C_{biv}(t) = C_b(t)$ for $t \geq \tau$, (28).

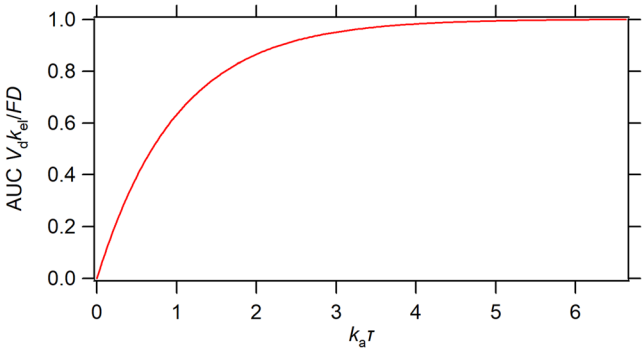

Fig. 1 Plot of $[AUC]_0^\infty k_{el}\ V_d/FD$ as a function of k_a and τ, (see Eq. 26).

we get:

$$Ge^{-k_{el}t} = C_b(\tau)e^{-k_{el}(t-\tau)}$$
$$= \frac{FDk_a}{V_d(k_a-k_{el})}\left(e^{-k_{el}\tau}-e^{-k_a\tau}\right)e^{-k_{el}(t-\tau)} \quad (29)$$

giving

$$G = \frac{FDk_a}{V_d(k_a-k_{el})}\left(e^{-k_{el}\tau}-e^{-k_a\tau}\right)e^{k_{el}\tau}$$
$$= \frac{FDk_a}{V_d(k_a-k_{el})}\left(1-e^{-(k_a-k_{el})\tau}\right) \quad (30)$$

Then, the curve for the hypothetical intravenous bolus administration of an equal dose would give:

$$[AUC_{iv}]_0^\infty = \frac{G}{k_{el}} = \frac{FDk_a}{V_dk_{el}(k_a-k_{el})}\left(1-e^{-(k_a-k_{el})\tau}\right) \quad (31)$$

Using Eqs. 26 and 31 one can find

$$F = \frac{[AUC]_0^\infty}{[AUC_{iv}]_0^\infty} = \left(1-\frac{k_{el}}{k_a}\right)\frac{1-e^{-k_a\tau}}{1-e^{-(k_a-k_{el})\tau}} \quad (32)$$

Where F is the fraction of dose absorbed since both oral and intravenous data rely on a single oral dose administration to an individual. However, if first-pass effect is not encountered then F in Eq.32 denotes the bioavailable fraction. The limit of Eq.32 for $\tau = 0$ (intravenous bolus dose) correctly predicts that F tends to 1 as k_a tends to a very large number. Visual inspection of Eq.32, reveals that F is fully dependent on the values of the rate constants k_a, k_{el} and τ. Hence, an estimate for F can be obtained, based on the estimates of these parameters derived from the oral experimental data.

METHODS

Simulations were performed using Eqs. 1, 2, 6, 16–22, and 26. Pharmacokinetic data were fit with the functional forms for drug concentration in the blood stream as a function of time given by the same equations. Standard least squares method was used in order to adjust model parameters to experimental data, cf., FD/V_d, k_{el} and τ for the $(PBFTPK)_0$ and FD/V_d, k_a,k_{el} and τ for the $(PBFTPK)_1$ model, respectively. User-defined functions were written for the Igor software package by Wavemetrics for both simulations and data fittings.

RESULTS-DISCUSSION

In the last twenty years or so, biopharmaceutical scientists gradually unveiled the complex nature of gastrointestinal drug absorption phenomena, e.g., drug solubilisation, supersaturation, drug dissolution, drug precipitation, the interplay of food with the various processes, (selective) permeability and drug ionization changes along the gastrointestinal lumen affecting all above processes. In our days, all these phenomena are interpreted (modeled) with the use of PBPK (physiologically based pharmacokinetic) models (13, 14). Undoubtedly, a single value of the absorption rate constant cannot capture the complex dynamics of the absorption phase phenomena taking place concurrently. It is worthy to mention that drug absorption is assessed in PBPK studies using the permeability estimate expressed in constant velocity units (length/time), i.e., "a zero-order type parameter". Likewise, drug absorption in the $(PBFTPK)_0$ models (7) is also expressed in constant mass/time units. For both $(PBFTPK)_0$ (7) and $(PBFTPK)_1$ (4–6) models the duration of the absorption process, τ, is a pivotal element. Similarly, the user/modeler of the software packages (GastroPlus® Software, n.d.; Simcyp® Simulator,n.d.; PK-Sim® Software, n.d.) of the PBPK (15, 16) (https://www.simulations-plus.com/software/gastroplus) models fix a finite time absorption period, e.g., 199 min (17) or transit times for each anatomical segment are specified (15, 16) (https://www.simulations-plus.com/software/gastroplus). In some cases (15), when PBPK models are coupled with a pharmacokinetic model the fraction of dose absorbed is related proportionally to drug concentration in the gastrointestinal lumen since "the blood on the basolateral side of the membrane is regarded as an ideal sink". Overall, the fixed time duration of the absorption processes (4–6, 15–17) and the deviations from the classical first-order absorption (4–6) have been adopted in the PBPK models (15).

(PBFTPK)0 and (PBFTPK)1 models: A pictorial comparison using simulations

Figures 2 and 3 show $(PBFTPK)_0$ and $(PBFTPK)_1$ models, respectively; for comparative purposes, curves generated from the classical Bateman equation (Eq. 1) without time restrictions are also shown in Fig. 3.

Figure 2A and B show a simple zero-order process (2A) and two successive constant input rates (2B), whereas the

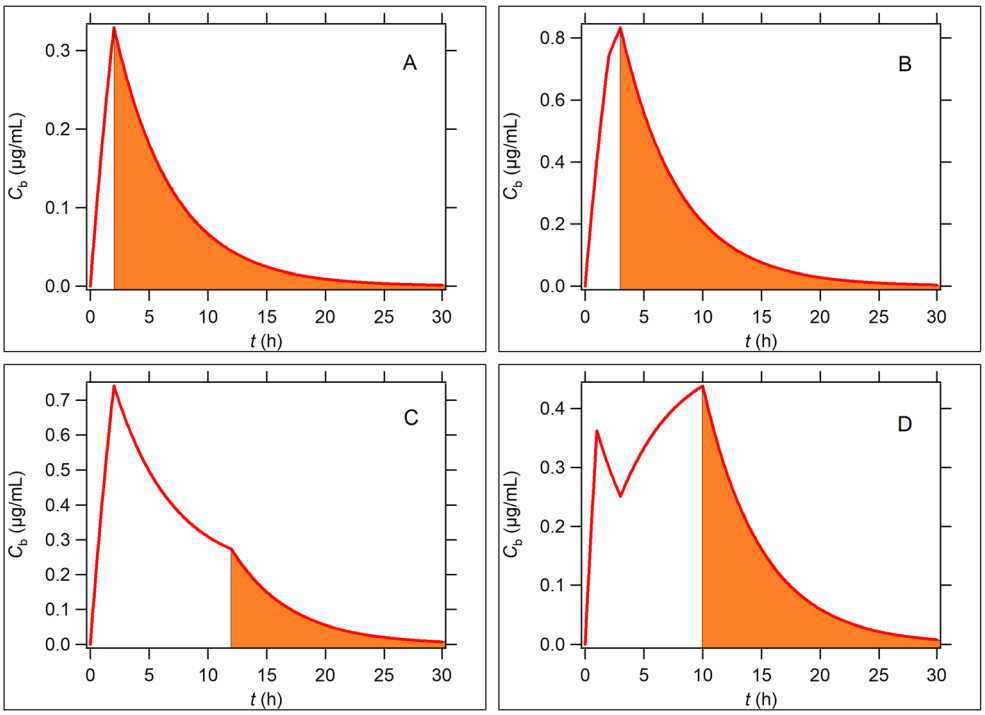

Fig. 2 Concentration *versus* time curves for $(PBFTPK)_0$ models. In all cases the value for k_{el} was set equal to 0.2 h^{-1} and V_d = 100 L. The absorption/elimination phase of curves in A, B, C, D, was generated using Eqs.6 and 2 and its variants Eqs. 16–22. A: $(FD/\tau) = 0.2$ mg/h, $\tau = 2$ h; B: $(F_1D/\tau_1) = 45$ mg/h, $\tau_1 = 2$ h and $(F_2D/\tau_2) = 25$ mg/h, $\tau_2 = 1$ h; C: $(F_1D/\tau_1) = 45$ mg/h, $\tau_1 = 2$ h and $(F_2D/\tau_2) = 4$ mg/h, $\tau_2 = 10$ h; D: $(F_1D/\tau_1) = 40$ mg/h, $\tau_1 = 1$ h and $(F_2D/\tau_2) = 0.5$ mg/h, $\tau_2 = 2$ h and $(F_3D/\tau_3) = 10$ mg/h, $\tau_3 = 7$ h. In all cases the red areas correspond to drug's elimination phase.

termination of the absorption process, τ, leads to $C_{max} = C_b(\tau)$. For these cases, (Fig. 2A and B), the equality $C_{max} = C_b(\tau)$ means that C_{max} is not a steady-state value described by Eq. 5, i.e., C_{max} corresponds to the termination of drug input, Eq. 7. In some cases, when a very highly soluble and permeable drug is studied, this type of C_b, t profiles (Fig. 2A and B) can indicate the completion and not simply the termination of drug absorption; plausibly, biowaivers can exhibit C_b, t profiles similar to Fig. 2A and B.

Figure 2C and D show two examples with two or three successive constant input rates, respectively. In both cases, the termination of drug absorption takes place in the colon ($\tau = 12$ h and $\tau = 10$ h), respectively which are longer than t_{max}. In Fig. 2C, C_{max} is higher than $C_b(\tau)$, since the termination of drug absorption lies in the descending portion of the elimination limb of the curve, $C_{max} > C_b(\tau)$. Figure 2D shows a simulated example with three constant input rates causing fluctuation of the drug concentration during the absorption/elimination phase. The second lower input rate can be associated with a lower segmental permeability and/or partial drug precipitation. Thus, the observed concentration maximum C_{max} is higher than the second peak ($C_b(\tau)$) associated probably with drug's re-dissolution and/or higher intestinal permeability. Again, C_{max} is not a steady-state value described by Eq. 5; in fact, C_{max} corresponds to an "equilibrium" point of the complex absorption phenomena in the small intestine.

The simulated examples of Fig. 2 demonstrate the rich dynamic behaviors associated with the $(PBFTPK)_0$ models. Most importantly, Fig. 2 shows that the relative magnitude of the parameters C_{max}, t_{max} *vis a vis* $C_b(\tau)$ and τ can vary remarkably according to the specific case examined. In all cases, however, the concentration of drug starts to decline monotonically beyond the datum point ($C_b(\tau)$, τ), i.e., drug absorption is not taking place beyond time τ.

Figure 3 shows simulated curves generated from $(PBFTPK)_1$ models. Three examples with various finite time absorption durations deviating from the classical first-order absorption (top curve in all graphs of Fig. 3) are shown using three different values of absorption rate constant k_a, namely, 0.1 h^{-1} (Fig. 3A), 0.25 h^{-1} (Fig. 3B), 0.5 h^{-1} (Fig. 3C). The curves corresponding to the lower value of the absorption rate constant 0.1 h^{-1} depicted in Fig. 3A clearly indicate that the smaller is the duration of the absorption time, the larger is the difference in the concentration-time profiles compared to the classical top curve. The examples shown in Fig. 3B and C using higher values for the absorption rate constant, 0.25 and 0.5 h^{-1}, respectively, demonstrate that the concentration-time profiles become progressively indistinguishable from the classical case (top curve) as the values of the duration of drug absorption, τ and the absorption rate constant k_a are increasing. These observations are in full agreement with Eq. 25 and the relevant plot of Fig. 1. It is worthy to mention that the classical top curve of Fig. 3A, exhibits appreciable drug absorption of drug beyond the physiological limit of 30 h (7) using the frequently encountered values for absorption and elimination rate constants, 0.1 and 0.05 h^{-1}, respectively. Accordingly, concern is rising

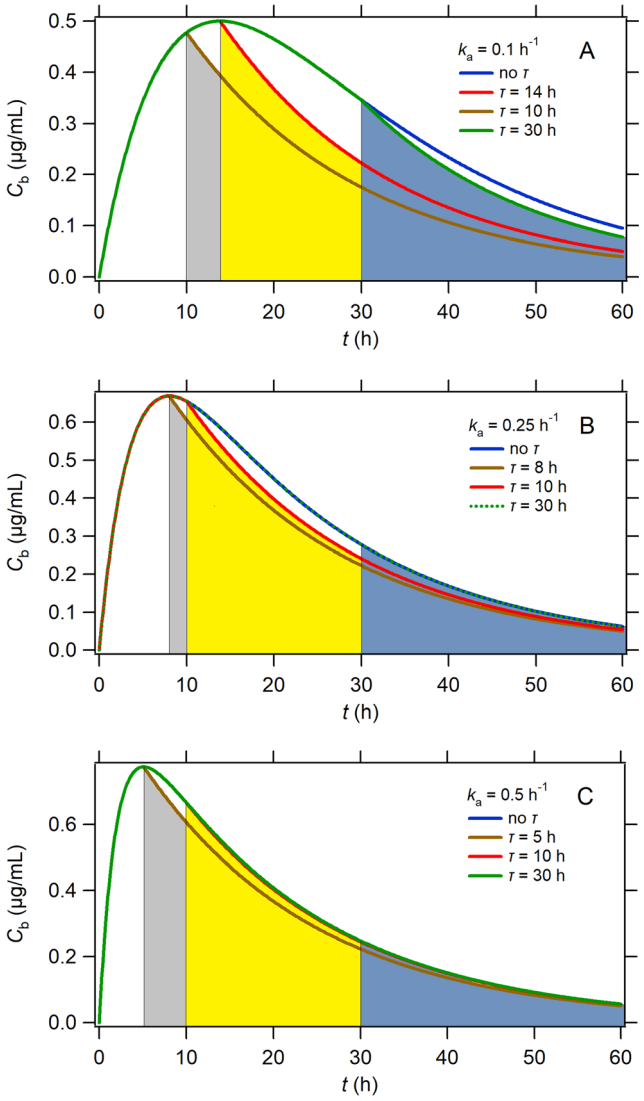

Fig. 3 Truncated Bateman drug concentration profiles with A: $k_a = 0.1\ h^{-1}$, $k_{el} = 0.05\ h^{-1}$ and termination times 10 h (gray), 14 h (yellow) and 30 h (blue); B: $k_a = 0.25\ h^{-1}$, $k_{el} = 0.05\ h^{-1}$ and termination times 8 h (gray), 10 h (yellow) and 30 h (blue); C: $k_a = 0.5\ h^{-1}$, $k_{el} = 0.05\ h^{-1}$ and termination times 5 h (gray), 10 h (yellow) and 30 h (blue).

for significant drug absorption beyond absorptive sites (4). According to Eq.26 the ratio of the area under the curve for τ values 14 and 30 h compared to the area of the top curve in Fig. 3A is 75 and 95%, respectively indicating that a misinterpretation for an infinite absorption is quite possible. Finally, the observations quoted above, which are associated with the relationship $C_{max} \geq C_b(\tau)$ for the $(PBFTPK)_0$ models shown in Fig. 2, are also applicable for the $(PBFTPK)_1$ models depicted in Fig. 3. Intuitively, one can conclude that the shorter is the absorption time duration τ, the higher is the resemblance of the concentration-time profiles generated from the $(PBFTPK)_0$, $(PBFTPK)_1$ models and the classical Bateman function (Eq.1). This is so since all curves approximate the limiting case, i.e., the intravenous bolus administration in one-compartment model.

Rate metrics: (C_{max},t_{max}) vis a vis ($C_b(\tau)$, τ)

The use of C_{max} as a measure of the rate of absorption is historically associated with its derivation from Eq.1 as a steady-state value. Although it is used as a bioavailability rate parameter, Eq.5 reveals that C_{max} is also dependent on the extent of absorption. During the previous decades concerns on this problem were raised and several alternative metrics and methodologies have been suggested (18–22). However, C_{max} is always being used as a rate parameter in all bioequivalence guidelines, but mainly its numerical value provides the maximum concentration of the drug in blood.

According to Eq.7 of $(PBFTPK)_0$ models, $C_b(\tau)$ is proportional to the rate of input FD/τ. This is an ideal property for a rate of input parameter; besides, time τ underlines the termination of the absorption process, which is the fundamental characteristic of the $(PBFTPK)_0$ models. Although C_{max} and $C_b(\tau)$ differ conceptually, in actual practice the two quantities may or may not be identical since $C_{max} \geq C_b(\tau)$, Fig. 2. When $C_{max} = C_b(\tau)$, one can easily derive from the $(PBFTPK)_0$ models (7).

$$Rate\ in = \frac{V_d C_b}{dt} = \frac{FD}{\tau} - k_{el} C_b V_d = 0 \tag{33}$$

$$C_b(\tau) = C_{max} = \frac{FD}{\tau k_{el} V_d} = \frac{FD}{\tau CL} \tag{34}$$

This equality means that the absorption of drug has been terminated or completed at time τ while C_{max} or $C_b(\tau)$ are proportional to the input rate (FD/τ) as well as to the extent of absorption (FD), Eq.34. However, C_{max} or $C_b(\tau)$ is not the asymptotic limit of a zero-order absorption process with first order elimination usually found as a steady-state solution in continuous intravenous infusion (12). In other words, the $(C_b(\tau),\tau)$ datum point is a discontinuity point associated with i) the completion of the input process (no more drug is available for absorption) or ii) a sudden change in drug's solubility, e.g., precipitation or iii) drug's permeability change, e.g., reduced regional permeability because of pH changes or iv) drug's transit beyond the absorptive sites.

The termination of absorption at time τ in the $(PBFTPK)_1$ models may result from the completion of drug absorption or the passage of drug beyond the absorptive sites. The corresponding value of $C_b(\tau)$ (Eq. 15), is always equal to or smaller than the experimental C_{max}, Fig. 3. However, the experimental values for $C_b(\tau)$ and τ of $(PBFTPK)_1$ models are not steady-state values, namely, C_{max} (Eq.5) and t_{max} (Eq.4), respectively; the pair $(C_b(\tau), \tau)$ represents a discontinuity time point.

Table I The ratio of $[AUC]_{\tau}^{72}$ of the test over the reference formulation of five pulmonary drugs and one oral drug in bioequivalence studies

PK parameters	Salmeterol (26)	Fluticasone (24)	Budesonide (25)	Formoterol (25)	Salmeterol (24)	Digoxin (27)
$\frac{([AUC]_{\tau}^{72})_{\text{test}}}{\left([AUC]_{\tau}^{72}\right)_{\text{reference}}}$	1.012	1.104	0.828	0.935	1.074	1.006
$\frac{([AUC]_{\tau}^{72})_{\text{reference}}}{\left([AUC]_{0}^{72}\right)_{\text{reference}}}$	0.987	0.858	0.977	0.994	0.935	0.958
$\frac{([AUC]_{\tau}^{72})_{\text{test}}}{\left([AUC]_{0}^{72}\right)_{\text{test}}}$	0.986	0.920	0.946	0.985	0.999	0.957

Exposure metrics: $[AUC]_0^{\infty}$ *versus* $[AUC]_0^{\tau}$ and $[AUC]_{\tau}^{\infty}$

The golden standard for the extent of absorption, without any doubt, in bioavailability-bioequivalence studies is $[AUC]_0^{\infty}$, Eq.2. This is also justified here for the $(\text{PBFTPK})_0$ models since the sum of Eqs. 8 and 9, adhering to the $(\text{PBFTPK})_0$ models principles, is equal to $[AUC]_0^{\infty}$, Eq.3. Although Eq. 8 reveals that $[AUC]_0^{\tau}$ is a fraction of $[AUC]_0^{\infty}$, its magnitude is solely determined from the quantity m, namely, the ratio of duration of the absorption process τ over the elimination half-life, $(m = \tau/t_{½})$. Therefore,the meaning of $[AUC]_0^{\tau}$ for the $(\text{PBFTPK})_0$ models is not in accord with the usual concept of partial areas used as indicators for the initial rate of exposure (19, 20, 22). Besides, $[AUC]_0^{\tau}$ for the $(\text{PBFTPK})_1$ models is dependent on τ (Eq. 24), while $[AUC]_0^{\infty}$ (Eq. 26) is also dependent on τ. Hence, for both $(\text{PBFTPK})_0$ and $(\text{PBFTPK})_1$ models the usual role of partial areas (portions of $[AUC]_0^{\tau}$) is not applicable due to the involvement of τ in the calculations.

According to Eq.9, $[AUC]_{\tau}^{\infty}$ is proportional to the fraction of dose absorbed, which is in the general circulation at time τ (12). This proportionality is valuable for bioequivalence studies when the duration of the absorption process is short or very short and the absorption phase data exhibit high variability; this is the case with inhalers (23–25) and nasal products (26). For these formulations, the test-reference comparison can be based on the area $[AUC]_{\tau}^{\infty}$ which is proportional to the fraction of dose absorbed being in the general circulation at time τ. Table I shows the results based on the analysis of $[AUC]_{\tau}^{\infty}$ for the test and reference formulations of three bioequivalence studies (23–25). All ratios $\left([AUC]_{\tau}^{72}\right)_{\text{test}} / \left([AUC]_{\tau}^{72}\right)_{\text{reference}}$ for the five drugs studied lie in the range 0.828–1.104. Although the 90% confidence intervals for the means were not constructed, these values lie in the range of 80–125% used in bioequivalence testing. Besides, the ratios $[AUC]_{\tau}^{72}/[AUC]_0^{72}$ for all drugs and formulations studied are in the range 0.858–0.999, Table I, which indicates that the area $[AUC]_{\tau}^{72}$ represents a very large portion (>80%) of the total area $[AUC]_0^{\infty}$. Since the variability of the experimental data in the ascending limb of the curve of the inhaled products is very high (23–25), while a dense sampling strategy is usually applied, the use of $[AUC]_{\tau}^{72}$ as an extent of absorption metric can lead to a smaller number of volunteers and a less dense sampling protocol in bioequivalence studies. Data on oral absorption of digoxin (27), which also exhibits fast absorption assuming $t_{\max} = \tau$, were analyzed in the same way and included in Table I. Additional relevant data from two nasal absorption studies were analyzed assuming $t_{\max} = \tau$ and presented in Table II.

Scientific-regulatory implications

In the light of $(\text{PBFTPK})_0$ and $(\text{PBFTPK})_1$ models, a reconsideration of the meaning and use of the typical bioequivalence parameters analyzed and presented (C_{max},t_{max} and partial areas) is required. This is summarized in Table III along with the meaning and potential use of the novel parameters $(C_b)_{\tau}$, τ, $[AUC]_{\tau}^{\infty}$. Undoubtedly, the duration of absorption τ plays a pivotal role in all novel parameters of both $(\text{PBFTPK})_0$ and $(\text{PBFTPK})_1$ models. Its use should follow the physiological time constrains for intestinal and colon absorption (7); its diversity is pictorially shown in Figs. 2 and 3.

The remarks quoted in Table III can guide regulatory agencies for potential changes in the assessment of bioequivalence studies. The utilization of the parameters τ and $[AUC]_{\tau}^{\infty}$ as well as the re-consideration of the partial area utility as a rate of exposure metric are the most challenging questions. In addition, the two recommendations of the current bioequivalence guidelines (9, 10), namely, i) "The sampling schedule should also cover the plasma concentration time curve long enough to provide a reliable estimate of the extent of exposure which is achieved if $[AUC]_0^t$ covers at least 80% of $[AUC]_0^{\infty}$ " and ii) the specific time limit of 72 h, for the calculation of total AUC, i.e., "AUC truncated at 72 h ($[AUC]_0^{72}$) may be used as an alternative to $[AUC]_0^t$ for comparison of extent of exposure as the absorption phase has been covered by 72 h for imme-

Table II The ratio of $[AUC]_\tau^{|4}$ of the test over the reference formulation in a nasal absorption bioequivalence study of budesonide (28) and $[AUC]_\tau^3$ or $[AUC]_\tau^4$ ratios (powder *vs.* solution) in a comparative systemic bioavailability study (29) of three nasal remimazolam (RMZ) formulations

PK parameters	Budesonide	PK parameters	RMZ (10 mg)	PK parameters	RMZ (20 mg)	RMZ (40 mg)
$\frac{([AUC]_\tau^{|4})_{test}}{([AUC]_\tau^{|4})_{reference}}$	1.024	$\frac{([AUC]_\tau^3)_{powder}}{([AUC]_\tau^3)_{solution}}$	1.226	$\frac{([AUC]_\tau^4)_{powder}}{([AUC]_\tau^4)_{solution}}$	1.422	2.118
$\frac{([AUC]_\tau^{|4})_{reference}}{([AUC]_0^{|4})_{reference}}$	0.942	$\frac{([AUC]_\tau^3)_{solution}}{([AUC]_0^3)_{solution}}$	0.831	$\frac{([AUC]_\tau^4)_{solution}}{([AUC]_0^4)_{solution}}$	0.854	0.858
$\frac{([AUC]_\tau^{|4})_{test}}{([AUC]_0^{|4})_{test}}$	0.944	$\frac{([AUC]_\tau^3)_{powder}}{([AUC]_0^3)_{powder}}$	0.893	$\frac{([AUC]_\tau^4)_{powder}}{([AUC]_0^4)_{powder}}$	0.858	0.904

diate release formulations", should be re-considered in view of the results of the present study. This is so since drug absorption beyond 30 h is not physiologically sound (7, 30). However, long half-life drugs may require extensive sampling design because of the very slow disposition characteristics. Overall, this first analysis and the above mentioned remarks will certainly need further investigation and may eventually lead to regulatory implications.

Towards the unthinkable: application of Eqs. 15 and 32 for the estimation of absolute bioavailability from oral data exclusively

In this section we analyze published data from a bioequivalence study with three formulations of theophylline (31). This historical first calculation of absolute bioavailability from oral data exclusively is applied to theophylline since its absorption is not problematic being a Class I drug (highly soluble, highly permeable) (31). We first analyzed the entire set of elimination phase data using a semi-logarithmic plot, Fig. 4. All plots are linear and the regression coefficients, R^2 found were 0.9995, 0.9997, and 0.9998 for formulations A, B and C, respectively. This verifies that the entire set of elimination phase data follows one-compartment model disposition. Then, an unrestricted non-linear least squares fit of the $(PBFTPK)_0$ model (Eqs. 6 and 2), $(PBFTPK)_1$ model (Eqs. 1 and 2), and Bateman equation (Eq.1 without time restriction) was applied, Fig. 5. The parameter estimates are listed in Table IV along with the calculated F values derived from Eqs. 15 and 32 adhering to the $(PBFTPK)_0$ and $(PBFTPK)_1$ models, respectively.

Excellent fits were observed for all data sets, Table IV. There is a minor superiority of Bateman function and the $(PBFTPK)_1$ model over the $(PBFTPK)_0$ model which is associated with the usually more erratic absorption phase whereas one or two data points deviate slightly from the $(PBFTPK)_0$ model fitting. However, Eq. 15 provides for F a single estimate, 0.97 for all formulations studied while the estimates for F based on Eq.32 are 1.04 for formulations A and B and 1.45 for formulation C. The latter numerical value originates from the poor estimate for τ, 2.93 (3.04) h derived from the $(PBFTPK)_1$ model fitting. It is very well known that estimates for F cannot be derived from the fitting of the Bateman function to oral data. Nevertheless, all three approaches demonstrate that theophylline absorption has terminated in the small intestine; however, the $(PBFTPK)_0$ and $(PBFTPK)_1$ model fittings clearly show *the complete absorption of theophylline in the small*

Table III The meaning of the classical and novel bioequivalence parameters in the light of $(PBFTPK)_0$ and $(PBFTPK)_1$ models

Parameters	Remarks
C_{max}, $C_b(\tau)$	When $t_{max} = \tau$, C_{max} is equal to $C_b(\tau)$; it corresponds to the blood concentration at the termination or completion of drug absorption at time τ. When $t_{max} < \tau$, then $C_{max} > C_b(\tau)$; C_{max} does not correspond to the termination or completion of drug absorption at time τ.
t_{max}, τ	When $t_{max} = \tau$, the recorded t_{max} corresponds to the termination or completion of drug absorption at time τ. When $t_{max} < \tau$, the numerical value of τ is the physiologically meaningful parameter, since it denotes the duration of the absorption process.
Partial areas (portions of $[AUC]_0^\tau$) (19)	For the $(PBFTPK)_0$ models, the magnitude of the areas (portions of $[AUC]_0^\tau$) depends exclusively on m, ($m = \tau/t_{½}$); therefore,these portions cannot be used as early absorption rate indicators. For the $(PBFTPK)_1$ models, the magnitude of the areas (portions of $[AUC]_0^\tau$) and the total area ($[AUC]_0^\infty$) are both dependent on τ, Therefore these portions, are not typical indicators of the early absosprtion rate.
$[AUC]_\tau^\infty$	Proportional to the fraction of dose absorbed and remaining in the body at time τ. It could be used instead of $[AUC]_0^\infty$ when very fast absorption is encountered.

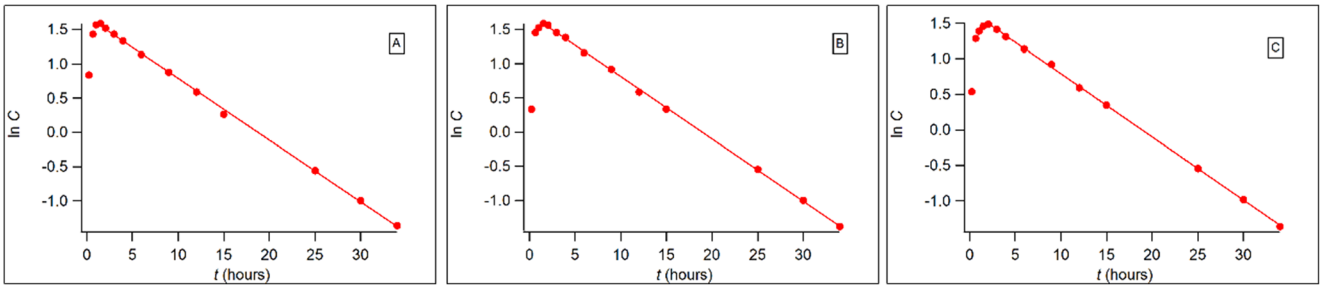

Fig. 4 Semi-logarithmic concentration-time plots of theophylline formulations A, B and C (32).

intestines from the three formulations studied. Needless to say that no clear advantage of the $(PBFTPK)_0$ and $(PBFTPK)_1$ models over the classical Bateman equation in terms of the modeling exercise could be concluded. This is so since the infinite time implied in the use of a first order input, everyone knows, never happens in the real world. The absorption process is almost completed after ca. 3 absorption half-lives. The remaining ca. 10% left to be absorbed is either not detectable or confounded by the experimental error. In practice, however, the use of the finite absorption time limit in the $(PBFTPK)_0$and $(PBFTPK)_1$ models allowed the estimation of F. This cannot be accomplished using the classical approach. The estimates for F derived in Table IV are in full agreement with the reported value for F, 0.96 ± 0.03 for immediate release theophylline tablets (32).

The simple example of theophylline analyzed belongs to the case of Class I drugs following one-compartment model disposition, simulated in Figs. 2A, B, 3A, B, whereas $C_{max} = C_b(\tau)$. However, caution should be exercised with the application of this method since most of the drugs exhibit two compartment model disposition while the complexity of drug transfer from the gastrointestinal tract to the systemic circulation and factors leading to interindividual variability (i.e., first pass effect, transporters, etc.) do not allow a valid estimation of F using Eqs. 15 and 32.

Estimation of F from oral data exclusively using a ratio of areas under the curve: For drugs obeying one compartment model

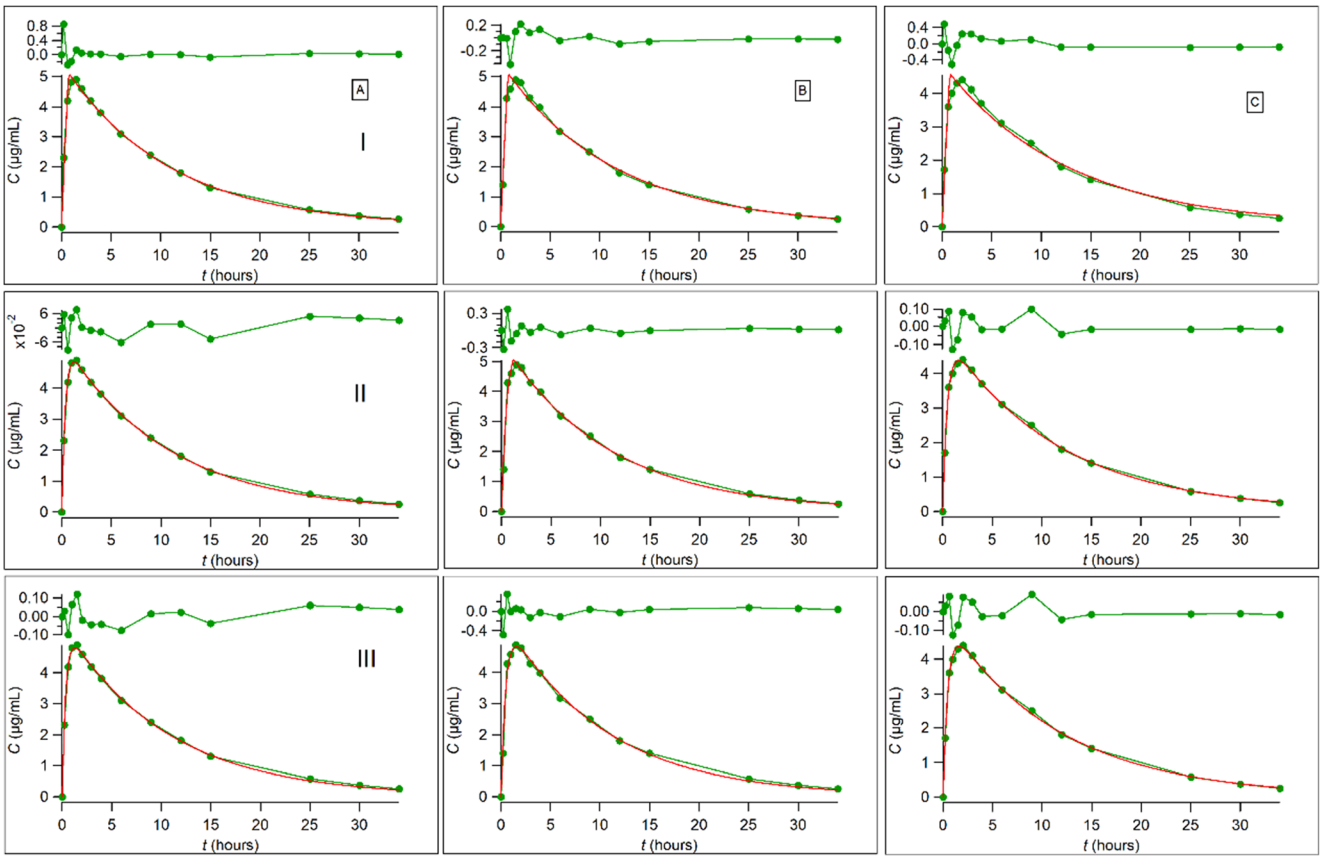

Fig. 5 Analysis of concentration time data of theophylline formulations A, B and C using the $(PBFTPK)_0$ model (Eqs. 6 and 2) (I), $(PBFTPK)_1$ model (Eqs. 1 and 2) (II), and Bateman eq. (III). Shown are the experimental data (31), model fit curves and residuals.

Table IV Parameter estimates (1 σ) derived from the fittings of $(PBFTPK)_0$ model (Eqs. 6 and 2), $(PBFTPK)_1$ model (Eqs. 1 and 2), and Bateman equation (Eq. 1 without time restriction) to experimental data (31), correlation coefficients for the fits and calculated bioavailable fraction *F*; the estimates for *F* designated F_{areas} are derived from Eq.36

Model	Formulation	FD/V_d (μg/mL)	k_a (h^{-1})	k_{el} (h^{-1})	τ (h)	R^2	F	F_{areas}
$(PBFTPK)_0$	A	5.29 (0.17)	-	0.092 (0.008)	0.72 (0.05)	0.990	0.967	0.960
	B	5.28 (0.09)	-	0.088 (0.004)	0.75 (0.03)	0.997	0.967	0.962
	C	4.73 (0.14)	-	0.079 (0.006)	0.76 (0.05)	0.989	0.970	0.959
$(PBFTPK)_1$	A	5.47 (0.09)	2.703 (0.122)	0.094 (0.002)	1.49 (0.30)	0.9997	1.043	-
	B	6.35 (0.66)	1.626 (0.329)	0.093 (0.005)	1.21 (0.18)	0.997	1.036	-
	C	5.03 (0.05)	2.062 (0.085)	0.087 (0.002)	2.93 (3.04)	0.9993	1.451	-
Bateman	A	5.42 (0.05)	2.776 (0.089)	0.096 (0.002)	-	0.9995	-	-
	B	5.63 (0.15)	2.072 (0.180)	0.098 (0.006)	-	0.996	-	-
	C	5.04 (0.05)	2.060 (0.069)	0.087 (0.002)	-	0.9993	-	-

disposition following any type of input kinetics lasting τ time units, an estimate for *F* can be also derived from the areas proportionality corrected in tems of dose:

$$F = \frac{[(AUC)]_{0\ oral}^{\infty} Dose}{\left[(AUC)_0^{\infty}\right]_{hy.i.v} \mathrm{FDose}} \tag{35}$$

where $\left[(AUC)_0^{\infty}\right]_{hy.i.v}$, (Fig. 6), corresponds to the area of the hypothetical intravenous bolus administration of the same dose derived from the back extrapolation of the elimination phase experimental data beyond time τ of the oral dose. Its numerical value is calculated from the ratio $e^{(y\ -\ intercept)}/k_{el}$, where the y-intercept on the *lnC* axis corresponds to the back extrapolated regression line with slope $-k_{el}$ of *lnC, t* elimination phase data beyond time τ. The integral $[(AUC)]_{0\ oral}^{\infty}$ is calculated using the trapezoidal rule from the experimental data, Fig. 6. Solving Eq.35 in terms of *F*,

$$F^2 = \frac{[(AUC)]_{0\ oral}^{\infty}}{\left[(AUC)_0^{\infty}\right]_{hy.i.v}} \tag{36}$$

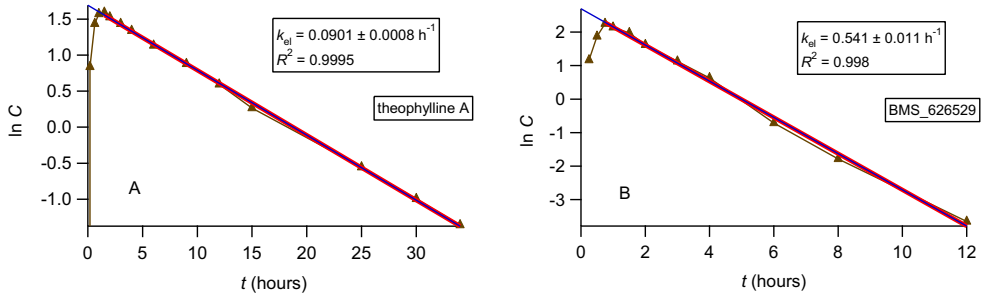

Fig. 6 Semilogarithmic plot of theophylline (A) from formulation A and BMS-626529 (B) plasma data. For both drugs the "triangle" represents the $\left[(AUC)_0^{\infty}\right]_{hy.i.v}$ semilogarithmically while the $[(AUC)]_{0\ oral}^{\infty}$ corresponds to the area under the curve of the experimental data points, depicted semilogarithmically too.

The positive root of Eq.36 provides the estimate for F. Eq.36 was used for the estimation of F of theophylline formulations, Table IV.The results show that very similar estimates were derived using the two methodologies, i.e., Eq.15 or 32 and Eq.36. Figure 6A shows the graphical analysis of a theophylline formulation. Besides, very similar results (not shown) were obtained using the experimtal $t_{\max}$ values of theophylline formulations instead of τ estimates. In this context, we analyzed the concentration plasma data of BMS-626529 drug (33) assuming $\tau = t_{max}$ and found $F = 0.904$, Fig. 6B.

We are currently working in order to develop methodologies and software for the estimation of absolute biovailability for all drug classes (I, II, III and IV) following one or two compartment model disposition. Preliminary simulation studies with two compartment model drugs show that the estimation of absorption duration, τ is problematic for drugs exhibiting very slow disposition in the body.

CONCLUSIONS

The realization that the gastrointestinal absorption takes place in finite time and the development of $(PBFTPK)_0$ and $(PBFTPK)_1$ models open a new era in the scientific and regulatory aspects of biopharmaceutical sciences. Several areas of research such as *in vitro in vivo* correlations, interspecies pharmacokinetic scaling will be affected beyond the fundamental bioavailability and bioequivalence topics. Most importantly, the estimation of absolute bioavailability from oral data exclusively can lead to regulatory implications.

Acknowledgments and Disclosures. Dedicated to the memory of Laszlo Endrenyi, a pioneer in bioavailability-bioequivalence research. Panos Macheras will use this paper as a plea for the minister of education of Greece to allow emeriti professors supervise undergraduates, MSc and PhD students after obligatory retirement. The authors wish to thank the anonymous reviewers for their constructive critique.

REFERENCES

1. Dost H. Der Blutspiegel. Kinetik der Konzentrationsverläufe in der Kreislaufflüssigkeit. Leipzig. 1953;
2. Tozer MR and T. Clinical Pharmacokinetics and Pharmacodynamics: Concepts and Applications. 4th ed. 2011.
3. Bonate PL. Pharmacokinetic-Pharmacodynamic modeling and simulation. 2nd ed. https://doi.org/10.1007/978-1-4419-9485-1, editor. Springer US
4. Macheras P. On an unphysical hypothesis of Bateman equation and its implications for pharmacokinetics. Vol. 36, Pharmaceutical Research. Springer New York LLC; 2019.
5. Sugano K. Lost in modelling and simulation? ADMET DMPK. 2021;9(2):75–109.
6. Sugano K. Biopharmaceutics modeling and simulations: theory, Practice, Methods, and Applications. 2012.
7. Macheras P, Chryssafidis P. Revising pharmacokinetics of Oral Drug absorption: I models based on biopharmaceutical/physiological and finite absorption time concepts. Pharm Res. 2020 Sep;37(10):187.
8. Amidon GL, Lennernas H, Shah VP, Crison JR. A theoretical basis for a biopharmaceutic drug classification: the correlation of in vitro drug product dissolution and in vivo bioavailability, Pharm res 12, 413-420, 1995–backstory of BCS. AAPS J. 2014;16(5):894–8.
9. Food and Drug Administration. Center for Drug Evaluation and Research (CDER). Waiver of In Vivo Bioavailability and Bioequivalence Studies for Immediate-Release Solid Oral Dosage Forms Based on a Biopharmaceutics Classification System. Guidance for Indust. 2017.
10. European medicines agency. Committee for medicinal products for human use (CHMP) guideline on the investigation of bioequivalence. London, Jan. 2017.Accessed March 10, 2021 2017.
11. Bateman H. The solution of a system of differential equation soccuring in the theory of radio-active transformations. Proc Cambridge Philos Soc Math Phys Sci [Internet] 1910;11(February):423–7. Available from: http://www.biodiversitylibrary.org/item/108210#page/35/mode/1up
12. Niazi S. Textbook of biopharmaceutics and clinical pharmacokinetics. 292 Madison Ave., New York
13. Charalabidis A, Sfouni M, Bergström C, Macheras P. The Biopharmaceutics Classification System (BCS) and the Biopharmaceutics Drug Disposition Classification System (BDDCS): Beyond guidelines. Int J Pharm [Internet]. 2019

May;566:264—281. Available from: https://doi.org/10.1016/j.ijpharm.2019.05.041.
14. Krzyzanski W, Jusko WJ, Wacholtz MC, Minton N, Cheung WK. Pharmacokinetic and pharmacodynamic modeling of recombinant human erythropoietin after multiple subcutaneous doses in healthy subjects. Eur J Pharm Sci Off J Eur Fed Pharm Sci. 2005;26(3–4):295–306.
15. Sjögren E, Westergren J, Grant I, Hanisch G, Lindfors L, Lennernäs H, et al. In silico predictions of gastrointestinal drug absorption in pharmaceutical product development: application of the mechanistic absorption model GI-Sim. Eur J Pharm Sci Off J Eur Fed Pharm Sci. 2013;49(4):679–98.
16. Certara Simcyp™ PBPK Simulator | Predicting drug performance.
17. Macheras P, Karalis V. A non-binary biopharmaceutical classification of drugs: the ABΓ system. Int J Pharm. 2014 Apr;464(1–2):85–90.
18. Endrenyi L, Fritsch S, Yan W. Cmax/AUC is a clearer measure than Cmax for absorption rates in investigations of bioequivalence. Int J Clin Pharmacol Ther Toxicol. 1991;29(10):394–9.
19. Chen ML. An alternative approach for assessment of rate of absorption in bioequivalence studies. Pharm Res. 1992;9(11):1380–5.
20. Chen M-L, Davit B, Lionberger R, Wahba Z, Ahn H-Y, Yu LX. Using partial area for evaluation of bioavailability and bioequivalence. Pharm Res. 2011 Aug;28(8):1939–47.
21. Macheras P, Symillides M, Reppas C. An improved intercept method for the assessment of absorption rate in bioequivalence studies. Pharm Res. 1996 Nov;13(11):1755–8.
22. Macheras P, Symillides M, Reppas C. The cutoff time point of the partial area method for assessment of rate of absorption in bioequivalence studies. Pharm Res. 1994 Jun;11(6):831–4.
23. Soulele K, Macheras P, Silvestro L, Rizea Savu S, Karalis V. Population pharmacokinetics of fluticasone propionate/salmeterol using two different dry powder inhalers. Eur J Pharm Sci [Internet]. 2015;80:33–42 Available from: http://europepmc.org/abstract/MED/26296862.
24. Soulele K, Macheras P, Karalis V. On the pharmacokinetics of two inhaled budesonide/formoterol combinations in asthma patients using modeling approaches. Pulm Pharmacol Ther. 2018 Feb;48:168–78.
25. Soulele K, Macheras P, Karalis V. Pharmacokinetic analysis of inhaled salmeterol in asthma patients: evidence from two dry powder inhalers. Biopharm Drug Dispos. 2017 Oct;38(7):407–19.
26. Bioavailability and Bioequivalence Studies for Nasal Aerosols and Nasal Sprays for Local Action. FDA Guidance. 2003.
27. Center for Drug Evaluation and Research, Digoxin Bioequivalency Review 76268, https://www.accessdata.fda.gov/drugsatfda_docs/appletter/2002/76268_Digoxin_Approv.pdf
28. do Carmo Borges N. C., Barrientos Astigarraga R., Sverdloff C. E., Borges B. C., Rodrigues Paiva T., Rebelo Galvinas P., Agnaldo Moreno R., Budesonide quantification by HPLC coupled to atmospheric pressure photoionization (APPI) tandem mass spectrometry. Application to a comparative systemic bioavailability of two budesonide formulations in healthy volunteers, J. Chromatography B 879, 236–242 (2010). https://doi.org/10.1016/j.jchromb.2010.12.003
29. Pesic M, Schippers F, Saunders R, Webster L, Donsbach M, Stoehr T. Pharmacokinetics and pharmacodynamics of intranasal remimazolam-a randomized controlled clinical trial. Eur J Clin Pharmacol. 2020;76:1505–16. https://doi.org/10.1007/s00228-020-02984-z.
30. Abuhelwa AY, Foster DJR, Upton RN. A quantitative review and meta-models of the variability and factors affecting Oral` Drug absorption-part II: gastrointestinal transit time. AAPS J. 2016 Sep;18(5):1322–33.
31. Meyer MC, Jarvi EJ, Straughn AB, Pelsor FR, Williams RL, Shah VP. Bioequivalence of immediate-release theophylline capsules. Biopharm Drug Dispos. 1999 Dec;20(9):417–9.
32. Hendeles L, Weinberger M, Bighley L. Absolute bioavailability of oral theophylline. Am J Hosp Pharm [Internet]. 1977;34(5):525–7. Available from. https://doi.org/10.1093/ajhp/34.5.525.
33. Brown J, Chien C, Timmins P, Dennis A, Doll W, Sandefer E, et al. Compartmental Absorption Modeling and Site of Absorption Studies to Determine Feasibility of an Extended-Release Formulation of an HIV-1 Attachment Inhibitor Phosphate Ester Prodrug. J Pharm Sci. 2013;102:1742–51. https://doi.org/10.1002/jps.23476.